The Development of LAPAN-A3 Satellite Off-Nadir Imaging Mission

Nova Maras Nurul Khamsah
Satellite Technology Center
Indonesia National Institute of Aeronautics and Space
Bogor, Indonesia
nova.maras@lapan.go.id

Satriya Utama
Satellite Technology Center
Indonesia National Institute of Aeronautics and Space
Bogor, Indonesia
satriya.utama@lapan.go.id

Rise Hapshary Surayuda
Satellite Technology Center
Indonesia National Institute of Aeronautics and Space
Bogor, Indonesia
rise.hapshary@lapan.go.id

Patria Rachman Hakim
Satellite Technology Center
Indonesia National Institute of Aeronautics and Space
Bogor, Indonesia
patria.rachman@lapan.go.id

***Abstract*—It is crucial for Indonesia as an agricultural country to have its own satellite image to be utilized in Indonesia's resources monitoring. LAPAN-A3 satellite data has been studied for earth observation and can be utilized for monitoring paddy fields, built-up areas, forests, rivers, fishponds, shrubs, sea, agricultural lands, and bare soils. But, as a sun-synchronous satellite, LAPAN-A3 has demerit of little revisit time for one specific area. Therefore, off-nadir imaging becomes one essential trait of the satellite to increase target monitoring from 17 times to 71 times in a year. This paper aims to organize the development process of off-nadir strategy in acquiring target image in Indonesia. With two kinds of off-nadir maneuver, inertial pointing maneuver and wheel speed maneuver, LAPAN-A3 satellite can conduct off-nadir imaging up to 34.5° roll angle maneuver. Furthermore, wheel speed maneuver with roll angle and roll rate approach presents the improvement in time efficiency of the maneuver, from 1 hour and 35 minutes executing time in inertial pointing to 25 minutes in wheel speed maneuver, making it become promising candidate for time-constraint off-nadir imaging.**

Keywords—earth observation, satellite maneuver, off-nadir imaging

I. INTRODUCTION

LAPAN-A3 is one of Indonesian microsatellites developed by National Institute of Aeronautics and Space (LAPAN) which has been orbiting since June 2016. LAPAN-A3 main mission is for earth observation, especially in Indonesia [1]. Therefore, one of the satellite main payloads is a multispectral imager used for remote sensing purposes. As Indonesia is a big country with many natural resources, acquiring data using satellite multispectral imager can be utilized to help national resources monitoring [2].

Indonesia is one of the big maritime countries with scores of active volcanoes, which is very liable to earthquake and tsunami. This makes the utility of satellite multispectral image of Indonesia can be exploited even more. The exercise of frequent satellite imaging using Indonesia's very own satellite will be able to support updating the condition of the disaster-prone area in Indonesia. Nevertheless, the imaging missions for LAPAN-A3 are not limited to Indonesia. As the satellite is orbiting in polar sun-synchronous orbit (SSO), LAPAN-A3 only passes Indonesia two to three times in the daytime. As a result, numerous chances to capture satellite images of other countries are openly wide.

Continuing the heritage from LAPAN-TUBSAT, the first Indonesian experimental microsatellite, and LAPAN-A2, the second generation yet the first satellite developed in Indonesia, LAPAN-A3 possesses similar actuators. LAPAN-A3 employs four reaction wheels and three magnetic torques using momentum biased attitude control [3], which utilized for satellite maneuver in imaging purposes. In conducting imaging missions, LAPAN-A3 satellite can exercise two modes, nadir mode, and off-nadir mode. Nadir imaging is a condition where imaging mission conducted along satellite ground track, while off-nadir imaging operated when the satellite needs to capture image far from its ground track.

Even though there are many advantages of the LEO sun synchronous satellite [4], the SSO satellite has a demerit of little revisit time for the areas of the interests within the equator region [5]. LAPAN-A3 satellite is competent to monitor one target 17 times a year in nadir mode and 71 times a year in off-nadir mode [6]. Therefore, off-nadir imaging becomes an essential trait of the satellite imaging missions. In conducting off-nadir imaging mission, LAPAN-A3 has developed two modes, inertial pointing maneuver, and wheel speed maneuver. This paper aims to introduce the off-nadir strategy of LAPAN-A3 satellite to optimize satellite off-nadir imaging missions.

This paper is organized into four main sections. Section II describes LAPAN-A3 system and utilization. Section III describes material and method used in this paper. Section IV describes the results and analysis. Section V describes the discussion of results.

II. LAPAN-A3 SYSTEM AND UTILIZATION

For fulfilling the observation missions, LAPAN-A3 equipped with two-star sensors, three fiber optic gyros, six coarse sun sensors, and one horizon sensor as attitude determination sensors. Also, four reaction wheels and three magnetic torques employed as actuators. These sensors and actuators comprise the attitude determination and control system (ADCS) of LAPAN-A3 [3]. Moment of inertia of LAPAN-A3 reaction wheel (I_w) is 0.00058, and moment of inertia of satellite is displayed in equation (1).

978-1-7281-3675-2/19/$31.00 ©2019 IEEE

$$I_{sat} = \begin{bmatrix} 5.79399 & -0.01848997 & 0.04966774 \\ -0.01848997 & 6.694604 & 0.00890283 \\ 0.0496674 & 0.00890283 & 5.097722 \end{bmatrix} \quad (1)$$

LAPAN-A3 implements the open-loop control system [7] with momentum-biased stabilization method for its operational nadir pointing. The reaction wheel on the pitch axis which is perpendicular to orbital plane absorbs the angular momentum of the satellite, while magnetic torques are used to maintain angular momentum vector to the desired magnitude and direction. By setting the angular velocity of the reaction wheel on the roll axis to zero, it can be used to reduce most of the nutation to a certain level [3].

Earth observation satellite, or a remote sensing satellite is a satellite which brings camera for earth observation mission to identify and map various object on Earth surface. There are four classifications of sensors for remote sensing; spatial, spectral, radiometric, and temporal [8]. The main payload of the LAPAN-A3 satellite is multispectral push-broom imager which using spectral resolution to describe the wavelength interval at which the observation initiated.

LAPAN-A3 as Indonesia's very own earth observation satellite gives many advantages for Indonesia as a large agricultural country. There are many studies for LAPAN-A3 multispectral imager data, where [9] utilized the satellite data from observing paddy fields to monitor the changes in land use, and [10] analyzed the data for land cover classification which is classified into five classes, water, bare land, agriculture, forest, and secondary forest. References [9][10] concluded that LAPAN- A3 imager data could be used as an addition to other medium-resolution remote sensing satellite data such as Landsat-8 to monitor rice growth phase, lake ecosystem, forest areas, mangroves, and palm trees.

Another utilization of LAPAN-A3 multispectral imager data is also for land use/land cover mapping. Land use/ land cover (LULC) data describes the vegetation, water, natural surface, and cultural features on the land surface. [11] stated that LAPAN-A3 data is fitted to extract ten different LULC classes, built-up areas, forests, rivers, fishponds, shrubs, wetland forests, rice fields, sea, agricultural land, and bare soil.

III. Material and Method

As stated in the previous section, one of the LAPAN-A3 satellite main missions is for earth observation using multispectral imager. Images captured by a multispectral imager can be well corrected if the attitude determination and control system (ADCS) of the satellite has high accuracy [7]. Hence, aside from the importance of increasing satellite capability of target acquisition, off-nadir imaging strategy is demanded to get a high-quality image. To acquire the off-nadir target, the satellite maneuver classified into two modes, inertial pointing maneuver, and wheel speed maneuver.

A. Inertial Pointing Maneuver

Inertial pointing maneuver is a satellite maneuver to obtain inertial pointing, which means controlling the satellite to point to specific or designated target in the inertial frame. To acquire inertial pointing, initially the satellite is assigned command 0º in all axis, then after some specific time, the satellite is maneuvered on pitch axis in accordance to target's latitude by allotting pitch angle command to y-axis, and lastly the satellite is maneuvered on its roll axis by giving roll angle command to x-axis as displayed in Fig. 1. Pitch angle (θ) calculation presented in (2) below.

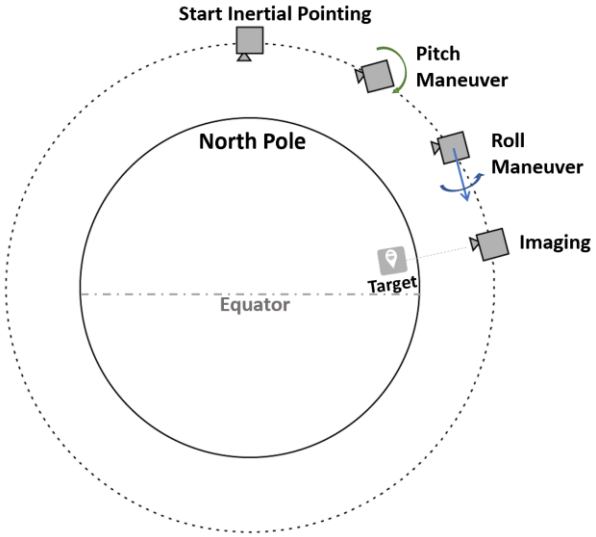

Fig. 1. Inertial Pointing Maneuver

$$\theta = \frac{\Delta t}{\tau} * 360^{\circ} \quad (2)$$

In the calculation of pitch angle, Δt is the time difference between time when satellite at the northern most (t_p) and time when satellite does the imaging (t_i) as explained in (3), and τ is the time period of LAPAN-A3 satellite.

$$\Delta t = t_i - t_p \quad (3)$$

While Fig. 2 illustrates the roll maneuver of the satellite, Fig. 3 points angular relationships between satellite, target, and earth center [12]. With R_E as Earth radius and H as the altitude of the satellite, the maximum elevation of the satellite (ρ) can be calculated in (4), while nadir angle (η) is acquired using (5) with λ as angular distance from subsatellite point (SSP) to the target.

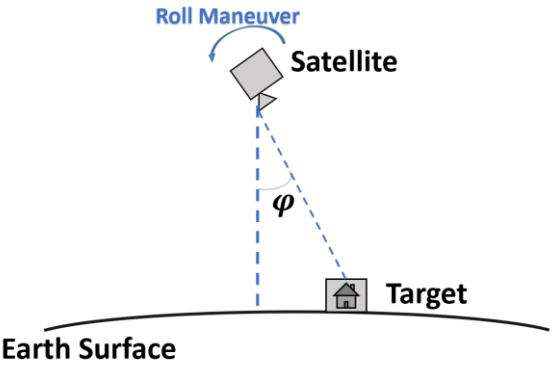

Fig. 2. Roll Maneuver

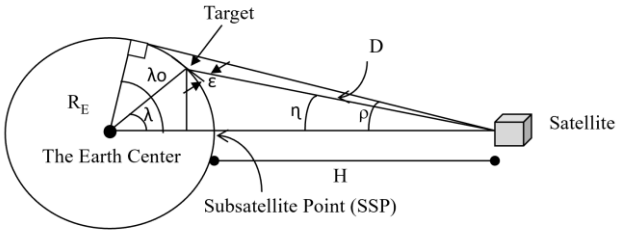

Fig. 3. Roll Calculation [11]

$$sin\,\rho = cos\,\lambda_0 = \frac{R_E}{R_E + H} \tag{4}$$

$$tan\,\eta = \frac{sin\,\rho\,sin\,\lambda}{1 - sin\,\rho\,cos\,\lambda} \tag{5}$$

Meanwhile, the relationship between satellite's elevation from target (ε) and Earth's angular radius (ρ), nadir angle (η) and angular distance (λ) is explained in (6) and (7) below.

$$cos\,\varepsilon = \frac{sin\,\eta}{sin\,\rho} \tag{6}$$

$$\eta + \lambda + \varepsilon = 90^o \tag{7}$$

The following equation calculates the range between satellite and the target (D).

$$D = R_E.\frac{sin\,\lambda}{sin\,\eta} \tag{8}$$

Roll maneuver of the satellite is to maneuver the satellite in the roll axis by giving roll angle command to the satellite, where the roll angle (φ) will be equal to nadir angle (η) when the range between satellite and the target (D) is minimum.

B. Wheel Speed Maneuver

Wheel speed maneuver is a satellite maneuver performed by operating the reaction wheel and allotting wheel speed command to spin the satellite. Because the angular momentum of the LAPAN-A3 satellite is coincided with pitch axis, to spin the satellite, the roll axis needs to be maneuver by giving roll angle command. Accordingly, the angular velocity existed in pitch axis needs to lessen, and the yaw axis needs to maneuver by given wheel speed command to stabilize the satellite.

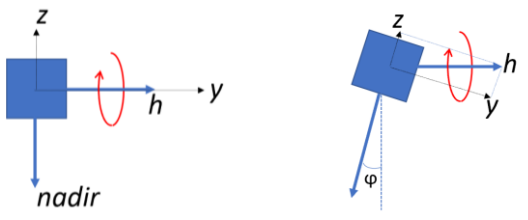

(a) (b)

Fig. 4 Attitude Satellite (a) Nadir Pointing, (b) Off-Nadir Pointing

Angular momentum ($\vec{h}$) of the satellite is obtained from the product of moment inertia of satellite wheel ($\vec{I_w}$) and angular velocity of the wheel ($\vec{\omega_w}$) added by the product of moment inertia of the satellite ($\vec{I_s}$) and angular velocity of the satellite ($\vec{\omega_s}$) as expressed in equation (9).

$$\vec{h} = \vec{I_w}\vec{\omega_w} + \vec{I_s}\vec{\omega_s} \tag{9}$$

As can be seen in Fig. 4 (a), in nadir pointing only Y component are existed, therefore the angular momentum is,

$$\overrightarrow{h_{nadir}} = I_{w.y}\omega_{w.y} + I_{s.y}\omega_{s.y} \tag{10}$$

with $I_{w.y}$ and $\omega_{w.y}$ represent moment inertia wheel y and angular velocity y respectively, and $I_{s.y}$ and $\omega_{s.y}$ stands for moment inertia satellite and angular velocity of satellite in y axis respectively. Meanwhile in off-nadir pointing as seen in Fig. 4 (b), due to the angular momentum ($\vec{h}$), Z component will emerge and will rotate the satellite. Hence, to nullify Z satellite rotation, wheel Z must be rotated.

$$\overrightarrow{h_{off-nadir}} = I_{w.y}\omega'_{w.y} + I_{w.z}\omega'_{w.z} + I_{s.y}\omega'_{s.y} \tag{11}$$

Wheel Z rotation can be calculated as follow,

$$I_{w.z}\omega'_{w.z} = \overrightarrow{h_{off-nadir}}\,\sin\varphi \tag{12}$$

In these maneuver, no external torque applied, so the angular momentum stays the same,

$$\overrightarrow{h_{off-nadir}} = \overrightarrow{h_{nadir}} \tag{13}$$

Therefore,

$$\begin{aligned} I_{w.z}\omega'_{w.z} &= \overrightarrow{h_{nadir}}\,\sin\varphi \\ I_{w.z}\omega'_{w.z} &= \left(I_{w.y}\omega_{w.y} + I_{s.y}\omega_{s.y}\right)\sin\varphi \\ \omega'_{w.z} &= \frac{I_{w.y}}{I_{w.z}}\omega_{w.y}\sin\varphi + \frac{I_{s.y}}{I_{w.z}}\omega_{s.y}\sin\varphi \end{aligned} \tag{14}$$

In Lapan-A3 all wheel has identical moment of inertia, thus equation (14) can be simplified to (15).

$$\omega'_{w.z} = \omega_{w.y}\sin\varphi + d \tag{15}$$

Variable d from (15) is negligible, so wheel Z rotation ($\omega'_{w.z}$) calculation can be expressed in equation (16).

$$\omega'_{w.z} = \omega_{w.y}\sin\varphi \tag{16}$$

With the similar approach, satellite angular velocity in Y axis must be compensated with,

$$\omega'_{s.y} = \omega_{s.y}\cos\varphi \tag{17}$$

Command sequence for wheel speed maneuver is developed into two approaches, roll angle and roll rate, as exhibited in table 1.

Table 1: Command Sequences of Wheel Speed Maneuver

Cmd	Approach			
	Roll Angle		Roll Rate	
	Pre-Imaging Commands	Post-Imaging Commands	Pre-Imaging Commands	Post-Imaging Commands
1	$Angle\ Z = 0$	$Angle\ Z = 0$	$Angle\ Z = 0$	$Angle\ Z = 0$
2	$Angle\ X = \varphi$	$Angle\ X = -\varphi$	$\omega'_{sx} = \omega_\varphi$	$\omega'_{sx} = -\omega_\varphi$
3	$\omega'_{s.y}$	$\omega_{s.y}$	$\omega'_{sx} = 0$	$\omega'_{sx} = 0$
4	$\omega'_{sx} = 0$	$\omega'_{sx} = 0$	$\omega'_{s.y}$	$\omega_{s.y}$
5	$\omega'_{w.z}$	$\omega'_{w.z} = 0$	$\omega'_{w.z}$	$\omega'_{w.z} = 0$

978-1-7281-3675-2/19/$31.00 ©2019 IEEE

Wheel speed maneuver requires five pre-imaging commands and five post-imaging commands. For pre-imaging, first the angle on the z-axis is valued to 0° ($Angle\ Z = 0$), then on the x-axis, the angle is set to a roll angle value ($Angle\ X = \varphi$) to roll the satellite for roll angle approach, or the angular velocity arranged to a roll rate value ($\omega'_{sx} = \omega_{\varphi}$) for roll rate approach. Following that, angular velocity existing in the y-axis should be compensated by given a compensated angular velocity ($\omega'_{s.y}$), and after the roll angle obtained, angular velocity in the x-axis fixed to 0°/s ($\omega'_{s.x} = 0$). Finally, to balance the maneuver, the z-axis is set to a new wheel speed ($\omega'_{w.z}$). For post-imaging, the commands are similar to pre-imaging commands, where the difference is in the command for the x-axis needs to be reversed ($Angle\ X = -\varphi$) for roll angle approach, and ($\omega'_{sx} = -\omega_{\varphi}$) for roll rate approach, also angular velocity in the y-axis is set back to the previous state called nadir mode ($\omega_{s.y}$).

Table 1 shows the difference between roll angle and roll rate approach, where the command number 2 is initially performed using angle command ($Angle\ X$), then in the roll rate approach it is developed into angular velocity command ($\omega'_{s.x}$). The calculation of roll angle (φ) refers to calculation in inertial pointing maneuver, as for the roll rate (ω_{φ}) is calculated using equation (18).

$$\omega_{\varphi} = \frac{\varphi}{t_{\varphi}} \tag{18}$$

where t_{φ} is stand for time needed to achieve roll angle φ.

The angular velocity of y axis ($\omega'_{s.y}$) on third command is calculated using equation (17), where $\omega_{s.y}$ is angular velocity of y in nadir mode. Then equation (16) explain the wheel speed of z axis ($\omega'_{w.z}$) calculation, with $\omega_{w.y}$ represent the wheel speed of y axis.

IV. Results and Analysis

Inertial pointing maneuver mode is the first mode which researched and developed for LAPAN-A3 satellite imaging mission. Fig. 5 display the image results of LAPAN-A3 satellite in conducting off-nadir imaging with ground track to target distance are 65 km or 7.2º roll angle, and 350 km or 34.5º roll angle respectively. From the explanation in the previous section, it is visible that the maneuver command sequence consists of practical commands and calculation. Nevertheless, the results of the maneuver displayed in Fig. 5 are satisfying, making this maneuver became one reliable maneuver mode.

To validate the results, Fig. 6 displayed the attitude of the satellite in roll axis when the satellite conducting off-nadir imaging Palu and Merbabu respectively. From the graphs, it is understood that roll maneuver of the satellite meet the need of the off-nadir requirements on each imaging missions, around 7.2º for Palu, and 34.5º of Merbabu. However, needs to be note that the roll angle is drifting at the time of acquisition.

Wheel speed maneuver is developed as a compliment to the established inertial pointing maneuver, therefore the maneuver are directed to acquire overseas images. Fig. 7 shows the result of wheel speed maneuver imaging mission in Djibouti and Suez.

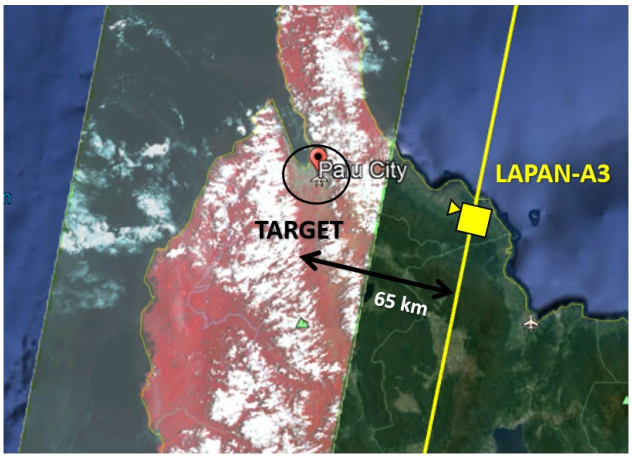

(a)

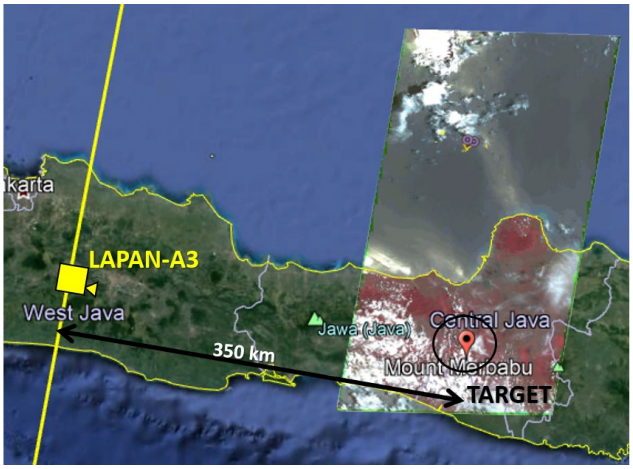

(b)

Fig. 5 Inertial Pointing Maneuver Images Result of LAPAN-A3 Satellite of (a) Palu, (b) Merbabu.

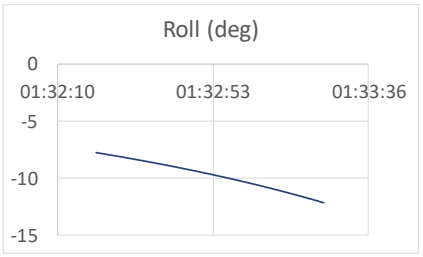

(a)

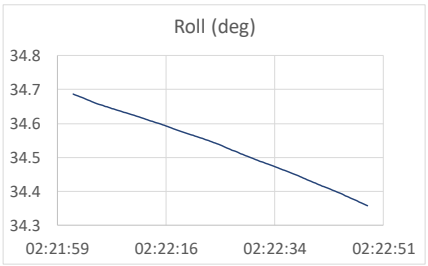

(b)

Fig. 6 Roll Angle of Off-nadir Imaging LAPAN-A3 Satellite of (a) Palu (Sulawesi), (b) Merbabu.

Both images are carried out more than 100 km maneuver distance, for about 11.8º roll angle for Djibouti, and 14.5º roll angle for Suez. Fig.7 alone can determine the result of wheel speed maneuver imaging, makes the maneuver become one reliable maneuver too for imaging missions.

Table 1 displays wheel speed command using two approach, roll angle command and roll rate command. The aim of both approaches is similar, which is to give roll maneuver. However, the roll angle command gives a direct command to the angle which can result in overshoot. This overshoot can be witnessed in the plot of roll angle in wheel speed maneuver of 20º roll in Fig. 8. From the comparison of Fig. 8 and Fig. 9, there is a slight difference. While in graph 3 using the roll angle command for roll maneuver, the roll target is obtained fast, means the wheel speed of roll axis is speedy, causes the overshoot in the target angle. In Fig. 9, the roll angle command is substitute by the roll rate command, creates stable wheel speed of roll axis, hence the smooth changes of the roll angle.

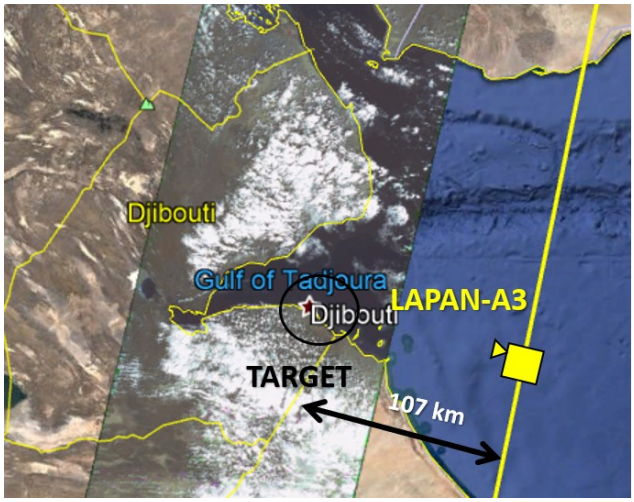

(a)

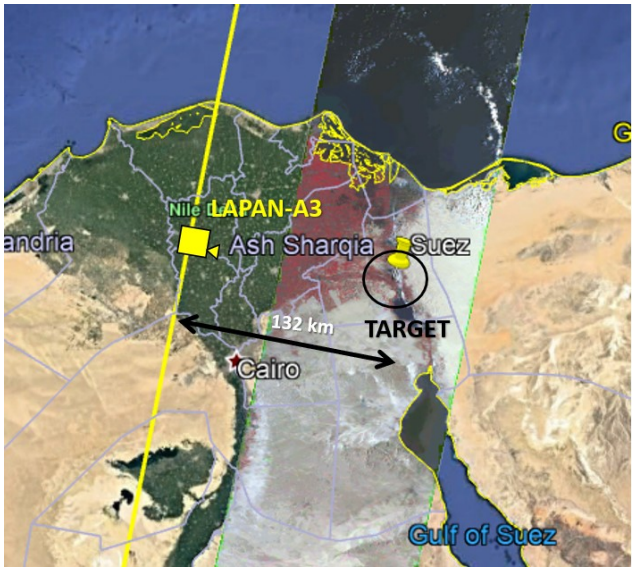

(b)

Fig. 7 Wheel Speed Maneuver Images Result of LAPAN-A3 Satellite of (a) Djibouti (b) Suez.

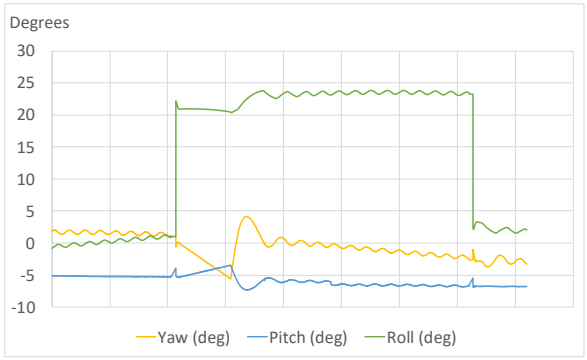

Fig. 8 Satellite Angle Plot of Wheel Speed Maneuver, Roll Angle Approach (Roll 20˚)

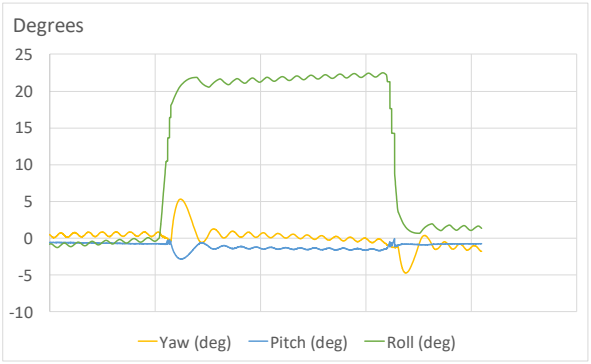

Fig. 9 Satellite Angle Plot of Wheel Speed Maneuver, Roll Rate Approach 0.3333º/s (Roll 20˚)

LAPAN-A3 multispectral image has field of view (FOV) 13.4º, hence to capture the area of interest, the offset of roll angle has to be below half of FOV (6.7º). From Fig. 8 and Fig. 9, it is shown that the roll angle achieved is not exactly 20º but in between 20º and 24º which means the offset is around 4º indicating a successful maneuver.

V. Discussion of Results

Table 2: Results Comparison from Fig. 6 and Fig. 7.

Maneuver	Target Image	Distance	Roll Angle *)	Results
Inertial Pointing	Palu	65 km	-7.2°	Target Acquired
	Merbabu	350 km	34.5°	Target Acquired
Wheel Speed	Djibouti	107 km	-11.8°	Target Acquired
	Suez	132 km	14.5°	Target Acquired

*) negative roll angle represents satellite roll to the west part from the ground track, and a positive roll angle represents satellite roll to the east part.

Table 2 displays a comparison between inertial pointing maneuver image results and wheel speed maneuver image results, both pleasing. Even though inertial pointing maneuver gives satisfying result, but the time of the maneuver is very stretched. The inertial pointing maneuver from the start to finish

978-1-7281-3675-2/19/$31.00 ©2019 IEEE

is conducted when the satellite is in the northern most, needed 1 hour 35 minutes in total. Meanwhile, time needed for the wheel speed maneuver commands is 7 minutes for pre-imaging mission, and 2 minutes for post-imaging mission, with the average of imaging missions around 20 minutes, the total time needed is only 29 minutes. Therefore, for the sake of time efficiency, the wheel speed maneuver is more promising than inertial pointing maneuver.

The wheel speed maneuver using roll rate approach also reduce the time needed for the maneuver to be conducted. The pre-imaging commands needed only 3 minutes to be executed and gives the total of 25 minutes for one off-nadir imaging mission. This can create the opportunity to exploit this maneuver for time-constraint imaging missions, for example in the case of multi-imaging mission in one orbital phase.

VI. Conclusion

This paper has organized the development of off-nadir maneuver for imaging mission of LAPAN-A3 satellite. As an earth observation satellite, it is important for the LAPAN-A3 satellite to conduct imaging missions. Therefore, to improve the ability to acquire a specific target, off-nadir imaging becomes one important facility of the satellite. Two modes of off-nadir maneuver that has been develop, inertial pointing maneuver and wheel speed maneuver, give splendid results. From the image results, inertial pointing maneuver can perform imaging mission from 7.2˚ to 34.5˚ roll angle maneuver, and the wheel speed maneuver can realize off-nadir imaging for 11.8º and 14.5º roll angle. However, for time efficiency, it is better to use the wheel speed maneuver which only needed 29 minutes for the maneuver to execute, than inertial pointing maneuver which requires 1 hour and 35 minutes. The wheel speed maneuver performed in two different approaches, roll angle command, and roll rate command, where roll rate command reduces the time of the maneuver even more, and gives smoother change in roll angle of the satellite.

One of off-nadir imaging applications is to support disaster monitoring as already performed in September 29th to October 11th, 2018 when LAPAN-A3 satellite support disaster monitoring in Palu, and could obtain Palu images 7 times, where the image can only be acquired one time in that period if only using nadir pointing imaging. This result encouraging the development of reliable off-nadir maneuver mode, and time-constraint supporting maneuver for future application.

Acknowledgment

Authors sincerely appreciate M.Mukhayadi, Ahmad Zammir Ribah, Sartika Salaswati, Annisa Sarah for their support and Satellite Technology Center, Indonesian National Institute of Aeronautics and Space for supporting this research.

References

[1] W. Hasbi and S. Suhermanto, “Development of LAPAN-A3 / IPB Satellite an Experimental Remote Sensing Microsatellite,” *Acrs 2013*, p. 4, 2013.

[2] C. T. Judianto and E. N. Nasser, “The Analysis of LAPAN-A3/IPB Satellite Image Data Simulation Using High Data Rate Modem,” *Procedia Environ. Sci.*, vol. 24, pp. 285–296, 2015.

[3] S. Utama, M. A. Saifudin, and M. Mukhayadi, “Momentum Biased Performance of LAPAN-A3 Satellite for Multispectral Pushbroom Imager Operation,” *IOP Conf. Ser. Earth Environ. Sci.*, vol. 149, no. 1, 2018.

[4] G. Taini, A. Pietropaolo, and A. Notarantonio, “Criteria and Trade-offs for LEO Orbit Design,” pp. 1–11, 2008.

[5] H. Septanto, S. Utama, R. H. Triharjanto, and Suhermanto, “Indonesia Coverage Simulation of SAR Satellite at Near-Equatorial Orbit,” *IOP Conf. Ser. Earth Environ. Sci.*, vol. 54, no. 1, 2017.

[6] P. R. Hakim and S. Utama, “Peningkatan Frekuensi Pencitraan Kamera Multispektral Satelit LAPAN-A3/IPB Menggunakan Manuver Pengamatan Off-nadir,” *Semin. Nas. Iptek Penerbangan dan Antariksa*, vol. XXi, pp. 28–38, 2017.

[7] P. R. Hakim, W. Hasbi, and A. H. Syafrudin, “ADCS requirements of Lapan-A3 satellite based on image geometry analysis,” *Proceeding - ICARES 2014 2014 IEEE Int. Conf. Aerosp. Electron. Remote Sens. Technol.*, pp. 142–146, 2014.

[8] G. Joseph, *Building Earth Observation Cameras*. New York: CRC Press Taylor & Francis Group, 2015.

[9] Y. Setiawan *et al.*, “Pemanfaatan Fusi Data Satelit Lapan-a3/Ipb Dan Landsat 8 Untuk Monitoring Lahan Sawah,” *J. Pengelolaan Sumberd. Alam dan Lingkung. (Journal Nat. Resour. Environ. Manag.*, vol. 8, no. 1, pp. 67–76, 2018.

[10] J. T. Nugroho, Z. Zylshal, and D. Kushardono, “Lapan-a3 Satellite Data Analysis for Land Cover Classification (Case Study: Toba Lake Area, North Sumatra),” *Int. J. Remote Sens. Earth Sci.*, vol. 15, no. 1, p. 71, 2018.

[11] Z. Zylshal, R. Wirawan, and D. Kushardono, “Assessing the Potential of LAPAN-A3 Data for Landuse/landcover Mapping,” *Indones. J. Geogr.*, vol. 50, no. 2, p. 184, 2018.

[12] H. Apgar *et al.*, *Space Mission Analysis and Design*. 1999.